

Very-low-frequency radio waves, once used only for long-range communications, are now used in a number of special applications. Two recent developments—long-range comparison of frequencies, and the investigation of the lower ionosphere by VLF phase measurements—are discussed in this paper. Some examples are given of the phase perturbations linked with Soviet high-altitude nuclear bursts of October 1962.

FREQUENCY MONITORING AND NUCLEAR BURST DETECTION

SOME ASPECTS OF VLF

C. R. Haave and B. W. Shaw

The Applied Physics Laboratory's interest in VLF (very-low-frequency) technology dates from 1960 when, in the development of the Navy's navigational satellite system, the need arose for a reliable and accurate means of checking reference oscillator frequencies at satellite-tracking stations throughout the world. Very-low-frequency monitoring was adopted for this purpose. By 1962, when the U. S. and Soviet high-altitude nuclear tests took place, VLF facilities at APL had expanded to provide continuous monitoring of all stabilized VLF transmissions then in existence. Thus it was that a substantial body of nuclear-burst-related VLF perturbation data also became available as a by-product of the system. Analysis of these data has pointed up some interesting and important connections between VLF perturbations and the trapped radiation from high-altitude nuclear bursts. It is the purpose of this article to describe briefly certain aspects of these developments at this Laboratory.

The VLF band of the radio spectrum is defined as extending over the frequency range of 3-30 kc/s; the corresponding wavelength range is 100-10 km, or about 54-5.4 n. miles. This frequency region was widely used for long-range

communication during the early days of radio, but was rapidly replaced by HF (3-30 mc/s), especially in the commercial services, after the HF band opened up in the 1920's. The higher frequencies, although less reliable, were more economical to generate than VLF, which required large, expensive antennas and transmitter installations (typical transmitter powers are of the order of hundreds of kw). Also VLF had the disadvantages of a relatively high natural noise background, narrow transmitting-antenna bandwidth and a small total available bandwidth.

In recent years, however, certain of the attractive features of VLF propagation, such as relative immunity to interruptions caused by ionosphere disturbances, penetration into seawater, and excellent phase stability, have led to a number of interesting applications. This has been especially true since the advent, in 1960, of VLF transmissions with carrier frequencies stabilized by atomic frequency standards. Among these applications, and apart from communication uses, are the long-range comparison of frequency standards, precision timing techniques, long-range navigational aids and the use of VLF as a tool for investigating the lower ionosphere. As we have already indi-

cated, VLF activities at APL have concentrated in the first and last of these areas. The Laboratory's VLF receiving equipment, frequency standards, and auxiliary apparatus needed for making VLF phase and amplitude measurements are housed in the Time and Frequency Standards Laboratory at the Howard County site of APL. Figure 1 is a photograph of the facility taken through the viewing window.

The large number of VLF papers that have appeared during the past five years is evidence of the widespread and growing interest in this subject. Some recent, exhaustive compilations are available,¹⁻⁴ in which particular aspects of VLF

can be pursued in more detail than is possible in this brief article.

Propagation of VLF

Very-low-frequency energy propagates in the spherical shell between the earth's surface and the lower ionosphere, with a mean effective ionosphere height of about 80 km. Its wavelengths (10-100 km) and the effective dimension of the waveguide are thus comparable, which means that ray-optics can describe the propagation only to a limited extent and that an exact solution is possible only with wave-optics, i.e. a complete solution of Maxwell's equations. This waveguide treatment of VLF propagation has come to be known as "mode-theory."

A plane waveguide with sharply bounded walls is already a complicated model. With consideration of earth curvature, ionosphere and ground parameters, mode excitation factors, and inhomogeneity and anisotropy of the ionosphere, a rigorous solution of the modal equation becomes a formidable mathematical task. Manageable working formulas are obtained only as approximate

¹ *A Bibliography of Unclassified Papers on Very Low Frequency Propagation*, Royal Aircraft Establishment Library Bibliography No. 251, Ministry of Aviation, London, 1964.

² "Symposium on the Ionospheric Propagation of VLF Radio Waves," *J. Res. Nat. Bur. Standards, Radio Science*, **68D**, Jan. 1964.

³ *Geophysical Effects of High-Altitude Nuclear Explosions of 1962*, compiled by E. J. Blau, APL Library Bulletin TG-230-B5, The Johns Hopkins University, Applied Physics Laboratory, Oct. 1, 1964.

⁴ *Propagation of Radio Waves at Frequencies Below 300 kc/s* (W. T. Blackboard, ed.), AGARD Ionospheric Research Symposium, Munich, 1962; and Macmillan Co., New York, 1964.

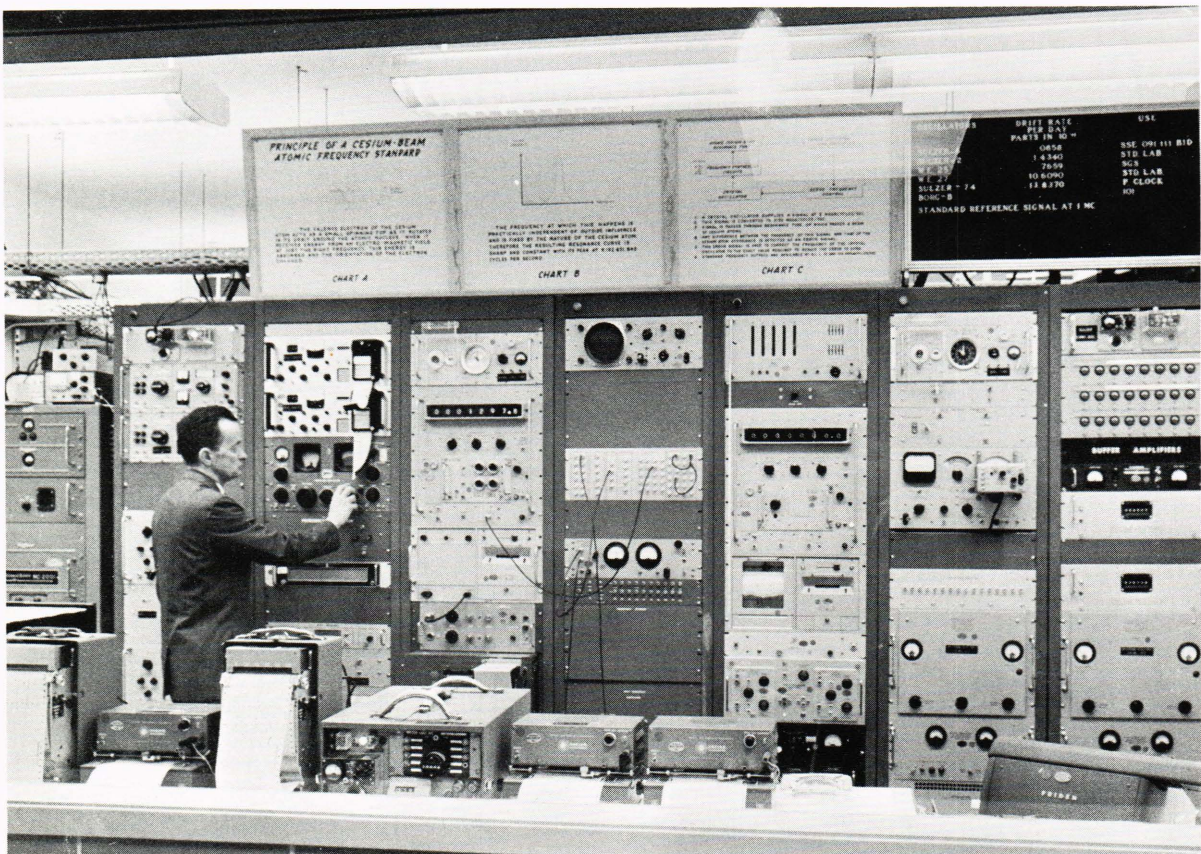


Fig. 1—APL Time and Frequency Standards Laboratory.

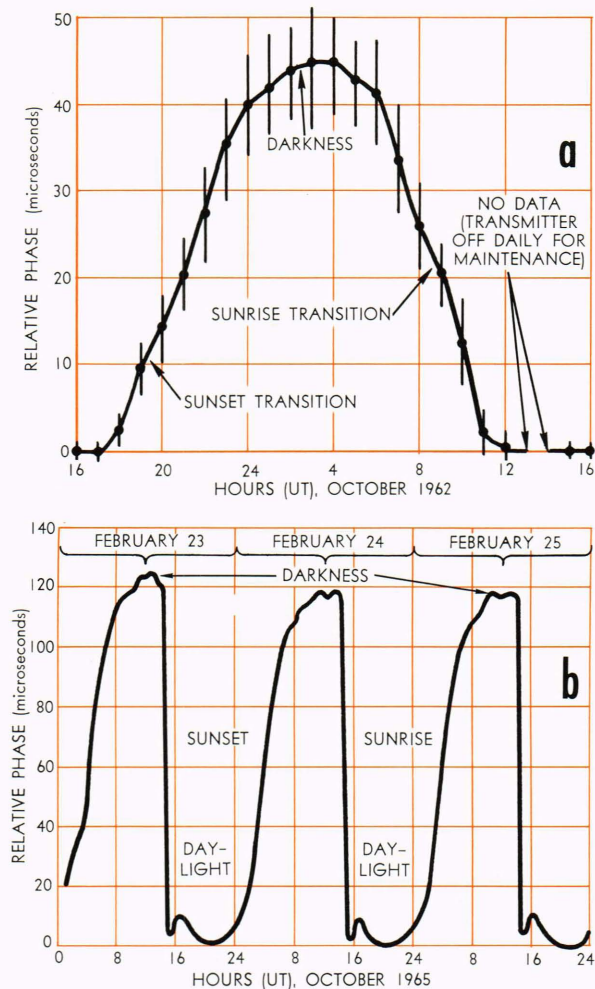


Fig. 2—Diurnal phase changes of VLF transmissions. (A) Mean diurnal phase change for the 16-kc/s transmission from GBR (Rugby, England). (B) Diurnal phase change for the 18.6-kc/s transmission from NLK (Jim Creek, Washington) as monitored by Satellite Tracking Station 019, McMurdo Sound, Antarctica, on Feb. 23, 24, and 25, 1965.

solutions. However, a number of useful results have been derived for some special cases and simplified approaches,^{5,6} in which VLF attenuation and phase characteristics are computed for various models of the lower ionosphere.

The source of VLF energy, a lightning discharge or a transmitting antenna, may be described in terms of a dipole, with an antenna size usually small with respect to the wavelength. For TM-modes, such as would be generated by a vertical

electric dipole, the waveguide in the VLF region is best represented if the ionosphere is considered to be a magnetic wall ($\mu \rightarrow \infty$) and the earth an electric wall ($\epsilon \rightarrow \infty$). The eigenvalues of the modal equation then determine the form and properties of the corresponding wave modes. Since a number of modes of significant energy will generally be propagated, the field at some distance from the transmitter is the vector sum of the contributions from the several modes. The higher-order modes, however, are attenuated more rapidly than is the first-order mode, so that at some range from the transmitter the contribution of the higher-order modes becomes small enough to be ignored for many purposes. The range at which this happens increases somewhat with frequency since the ratio of the attenuation of the higher-order modes to that of the first-order mode decreases with increasing frequency. The higher frequencies in the VLF band are thus more subject to irregularities due to mode interference, particularly during transient conditions (such as sunrise) over the propagation path. Near the middle of the band, say near 16 kc/s, propagation is essentially first-mode beyond about 4000 km.

The effective reflecting height of the ionosphere for VLF varies with solar illumination between about 70 km during all-daylight conditions and perhaps 90 km for all-darkness conditions, heights that are typical of the ionosphere D-region. (Actual heights will vary somewhat with frequency, path location on the earth's surface, and ionosphere state.) The effective dimension of the waveguide thus changes diurnally by about 20 km, and this effects a diurnal variation in the phase of the received signal. The magnitude and detailed nature of the diurnal phase change are functions of frequency, path length between transmitter and receiver, geometry and nature of the path on the earth's surface, time of year, and of various perturbing factors that can change the electrical properties of the lower ionosphere. The details of the phase cycle are in general not easily predictable; each specific VLF path has its characteristic diurnal "signature," which changes somewhat with season but usually preserves its characteristic features.

To illustrate this diurnal phase change, Fig. 2A shows the mean diurnal phase variation for GBR (Rugby, England, 16 kc/s) for Oct. 1962, as compiled from hourly values taken from continuous phase recordings made at the APL Time and Frequency Standards Laboratory. Figure 2B shows the diurnal phase change for the transmission from NLK (Jim Creek, Washington, 18.6 kc/s) as monitored by Satellite Tracking Station

⁵ J. R. Wait, "Influence of the Lower Ionosphere on Propagation of VLF Waves to Great Distances," *J. Res. Nat. Bur. Standards, Radio Propagation*, **67D**, July-Aug. 1963, 375-381.

⁶ H. Volland, "Zur Theorie der Ausbreitung langer elektromagnetischer Wellen," *Arch. Elektr. Übertragung*, **18**, 1964, 95-104, 181-188.

019 at McMurdo Sound, Antarctica, for Feb. 23, 24, and 25, 1965.

The total night-to-day phase shift for the GBR transmission (Fig. 2A) is seen to be about 45 μ sec. The vertical lines show the total spread observed in the GBR phase readings for that hour throughout the month; the spreads are actually somewhat smaller than shown, particularly during the sunrise and sunset transitions, because the values have not been adjusted for the changes in times of sunset and sunrise during the month. However, the general regularity of the diurnal change is clear, as is the excellent stability of the D-layer from day to day during the daylight hours. (This is the salient fact of VLF propagation, which makes VLF so useful as a stable propagation link in the long-range comparison of frequencies.)

This day-to-day repeatability is also evident in the three consecutive diurnal phase curves for the NLK-to-McMurdo Sound path shown on Fig. 2B. The total diurnal shift is seen to be about 120 μ sec for this path at this time of year.

Both of these paths are "long" paths in the sense that high-order modes should not be present in significant amounts. First-order mode theory predicts for such paths that at a given frequency the total diurnal shift should increase linearly with range, or the ratio $\Delta t/D$ (Δt is the total diurnal shift in μ sec, and D is the range in Kkm) should be constant. These ratios for these two specific paths and times of year are tabulated below.

Path	Frequency (kc/s)	Range (Kkm)	Δt (μ sec)	$\Delta t/D$ (μ sec/Kkm)
GBR-APL	16	5.8	45	7.7
NLK-McMurdo Sound	18.6	14.8	120	8.1

Values of $\Delta t/D$ of this order are typical for frequencies near the middle of the VLF band. Figure 3 shows some ranges of total diurnal phase shift that have been observed for long paths for NBA (Canal Zone, Panama, 18 kc/s) and GBR. The straight line ($\Delta t/D = 7.8$) was calculated from an expression for the difference between the daytime and nighttime phases of the first mode derived from the formulation of H. Volland:⁶

$$\Delta\phi \approx -\pi\rho(h_n - h_d) \left(\frac{\lambda}{16} \frac{h_n + h_d}{(h_n h_d)^2} + \frac{1}{\lambda a} \right),$$

in which $\Delta\phi$ is the phase difference in radians, ρ the range in km, h_n and h_d the nighttime and daytime ionosphere heights, λ the wavelength, and a

the earth's radius. The calculated curve is for a frequency of 17 kc/s and assumed ionosphere heights of $h_n = 90$ km and $h_d = 70$ km. The general agreement between the values predicted by first-order mode theory and the observed diurnal shifts in this frequency region is clear. The observed spreads in diurnal shift come about because the state of the ionosphere changes with both geographical location and season. However, while first-order mode theory predicts that the values of $\Delta t/D$ should decrease with increasing frequency throughout the VLF band, experimental data now becoming available on some paths for frequencies between 20 and 30 kc/s, toward the upper limit of the VLF region, suggest that $\Delta t/D$ reaches a minimum somewhere in the 16-20-kc/s region and again increases at the higher frequencies, even for "long" paths, indicating that first-order mode theory may not be adequate to describe propagation at these higher frequencies. It is perhaps significant that a quantitatively established waveguide theory for LF, just above the VLF region in frequency, is not available.

At ranges below about 4000 km, where substantial energy may exist in the higher-order modes, the values of total diurnal shift, as measured over various paths, show considerable deviation from the values predicted on the basis of first-order mode theory. Also, for some short paths the total diurnal shift may not repeat closely from day to day, probably because of instability in the relationships between the various modes present; such paths must be used with care in such applications as frequency monitoring, which depend on stable day-to-day phase relationships. It is also noted that long VLF paths over Arctic regions do not show a total diurnal phase change

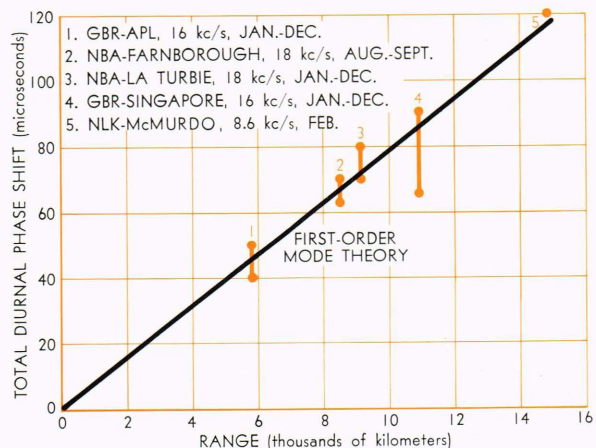


Fig. 3—Diurnal phase change as a function of range for long paths in the 16-18 kc/s region.

proportional to total path length, since often only a portion of the path length undergoes the diurnal change in illumination. The total diurnal change in these cases is proportional to that length of path actually subject to the diurnal solar illumination cycle.

Some other propagation factors characteristic of VLF should also be mentioned.

1. It has been established that a nonreciprocity exists between east-to-west and west-to-east propagation in that the attenuation is measurably less for west-to-east transmission. The nonreciprocity stems from interaction of the VLF wave and earth's magnetic field. Nonreciprocity in phase velocity, however, is apparently very slight.

2. Attenuation losses over a given VLF path are usually some few db less for all-darkness propagation than for all-daylight conditions. Normal daytime attenuation rates are of the order of 2-5 db/Kkm; the lower value pertains to over-water propagation, the higher values to mixed water-land, or all over-land, paths. Attenuation rates over special areas, such as permafrost regions, may be several times the normal rate.

3. VLF is subject to phase perturbations caused by any sporadic geophysical event that can alter the state of the lower ionosphere. Such perturbations are superimposed on the normal diurnal phase shift. Some known causes of propagation irregularities are volume ionization in the lower ionosphere associated with meteor showers, ionosphere irregularities accompanying magnetic storms, abnormal ionization in the D-region as a result of solar flares, and the electromagnetic and particle flux from high-altitude nuclear bursts.

Frequency Monitoring

Apart from communications uses, frequency monitoring is at present perhaps the most widespread application of VLF; the seven VLF stations now operating, with carrier frequencies stabilized to within one part in 10^{10} , provide essentially world-wide coverage for this purpose. In practice, the phase of the received VLF signal is compared with the phase of the local reference oscillator over some averaging period. Since in general the received phase of the VLF signal will contain phase changes due to propagation factors (such as the diurnal phase cycle described earlier, or phase irregularities resulting from ionosphere disturbances) some method must be devised to eliminate these factors from the oscillator comparison so that we can isolate the phase difference resulting solely from the oscillators being compared. A convenient way of doing this simply is made possible

by the nature of VLF propagation itself—the extremely good stability of the VLF phase from day to day during daylight hours.

To take advantage of this fact, the basic measurement that is made is the 24-hr comparison. In this measurement the mean relative frequency difference $\overline{\Delta f}/f$, between the local reference oscillator and the VLF transmission during the 24-hr period of comparison, is given by

$$\overline{\Delta f}/f = \Delta t/T,$$

where f is the nominal frequency, Δt is the change in phase (in μsec) of the received signal relative to the local reference that is accumulated in 24 hr, and $T = 8.64 \times 10^{10}$ (the number of μsec in a day). Such measurements are made with a phase-tracking VLF receiver that furnishes a continuous analog record of the relative phase of the VLF signal and that may also display the relative phase (in μsec) on a counter dial. The measurement is normally made each day at mean noon on the propagation path. As seen from Fig. 2, relative VLF phase variations from day to day do not normally exceed some few μsec during daylight hours. If, for example, we take 2 μsec as that part of Δt caused solely by propagation variations from day to day, $\overline{\Delta f}/f = 2.3 \times 10^{-11}$, which is about the limit of the system as set by propagation. Comparison to one part in 10^{10} , however, is to be expected routinely from the 24-hr comparison. Frequency comparisons can, of course, be made over shorter periods of time or between other times of day, but in general the accuracy will be degraded.

The Applied Physics Laboratory uses this VLF technique as a means of checking station reference oscillator frequencies at each of about 18 of the Navy's satellite-tracking stations located throughout the world. All VLF transmissions are continuously received at APL to tie this network together and to monitor propagation and transmission irregularities that may occasionally degrade the measurements. Results of these observations are transmitted daily to the network of tracking stations and to several other interested activities.

Since it is not feasible for all of the satellite-tracking stations to monitor the same VLF station, the APL facility keeps complete frequency logs on each VLF station in use. The measurements made by field stations using different VLF stations can then be coordinated properly. As an example of the records kept, Fig. 4 shows a plot of the 7-day mean frequency offsets from nominal for three VLF stations for the period from Nov. 17, 1964 through Apr. 13, 1965. It is seen that during

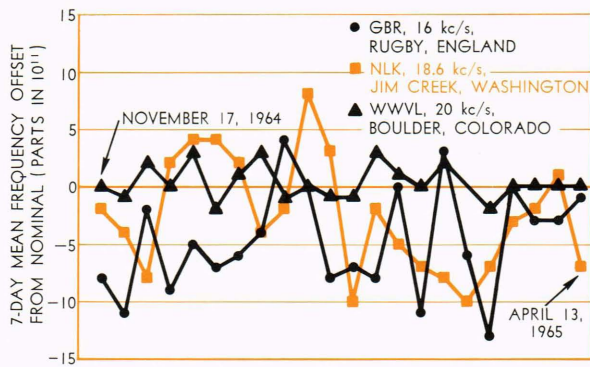


Fig. 4—Offsets from nominal frequency for some typical stabilized VLF transmissions.

this period the WWVL (Boulder, Colorado, 20 kc/s) carrier was held consistently to within 3 parts in 10^{11} of its nominal frequency. The other two stations (NLK and GBR) show somewhat greater dispersion than this; however, during the entire period NLK deviated from nominal by as much as 10 parts in 10^{11} only twice, and GBR only three times, when it was low by 11, 11, and 13 parts in 10^{11} , respectively.

VLF Phase Perturbations and Ionosphere Irregularities

The sensitivity of the VLF phase to relatively small changes in the state of the lower ionosphere, coupled with phase-stable transmissions and precise monitoring techniques, makes VLF phase-monitoring a valuable tool for investigating irregularities in the ionosphere D-region. The electron density at D-layer altitudes is only of the order of several hundred to 10^3 electrons/cc, so that probing by conventional sounding methods is relatively difficult. It is not known precisely how sensitive is the VLF phase to changes in electron density, but estimates have been made that changes of from one to several electrons/cc are detectable.

Thus any geophysical event capable of changing the electron density over an appreciable volume in the lower ionosphere will be detected as a "phase anomaly" superimposed on the regular diurnal phase change described earlier. One such event frequently observed is the solar flare, certain types of which give rise to sudden ionospheric disturbances. The ionization enhancement in the D and lower-E regions is due mainly to soft X-rays in the $1\text{-}10\text{\AA}$ band that are emitted as *bremstrahlung* from free electrons in the solar chromosphere. The height profile of the ioniza-

tion enhancement depends on the energy spectrum of the ionizing radiation, which varies from flare to flare. Very intense flares are accompanied at times by cosmic radiation enhancements (solar proton events), which can cause prolonged abnormal conditions in the lower ionosphere; this type of flare-connected perturbation may also affect VLF paths in the dark hemisphere, whereas the usual flare is observed only on VLF paths in the sunlit hemisphere. Such special events are rare (only about 10 had been observed up to 1960) and are observed primarily at the higher latitudes during times of maximum sunspot activity.

A typical flare-related VLF phase perturbation is characterized by a sudden phase advance (lowered effective ionosphere height) followed by a gradual recovery that may last an hour or more.

Very-low-frequency phase anomalies linked to such magnetic disturbances as magnetic storms or magnetic bay* events are usually not as clearly delineated in the phase record as are those accompanying solar flares. They are detected, for the most part, as irregular phase fluctuations, particularly in the nighttime phase, that may persist for several days for large storms. Magnetic bay events, however, have been observed to cause large daytime phase irregularities as well, during the time of high magnetic activity. It is important to be able to identify such events, since they represent "noise" in most applications of VLF.

Nuclear Bursts

A somewhat similar but man-made source of lower-ionosphere perturbations is the high-altitude nuclear burst. This Laboratory has been active in the investigation of these phenomena since the United States and Soviet test series in 1962. Some VLF observations made on this country's *STARFISH* burst of July 9, 1962, were reported in an earlier issue of the *Digest*,⁷ and this and other bursts of the U. S. test series were treated in subsequent publications.⁸⁻¹⁰

* A magnetic bay is a smoothly-varying temporal deviation of the geomagnetic field from its normal value, that lasts from one to two hours.

⁷ C. R. Haave, A. J. Zmuda, and B. W. Shaw, "VLF Phase Perturbations Associated with High-Altitude Nuclear Bursts," *APL Technical Digest*, 2, Nov.-Dec. 1962, 14-19.

⁸ A. J. Zmuda, B. W. Shaw, and C. R. Haave, "Very Low Frequency Disturbances and the High-Altitude Nuclear Explosion of July 9, 1962," *J. Geophys. Res.*, 68, 1963, 745-758.

⁹ A. J. Zmuda, B. W. Shaw, and C. R. Haave, "VLF Disturbances Caused by the Nuclear Detonation of October 26, 1962," *J. Geophys. Res.*, 68, 1963, 4105-4114.

¹⁰ A. J. Zmuda, B. W. Shaw, and C. R. Haave, "VLF Disturbances Caused by Trapped Beta-rays from the Decay of Neutrons Produced in High-Altitude Nuclear Explosions," *J. Res. Nat. Bur. Standards, Radio Science*, 68D, 1964, 117-123.

Very-low-frequency phase perturbations stemming from nuclear bursts occur not only in areas directly exposed to electromagnetic and particle flux from the burst, but also at remote locations where the entire VLF propagation path is shielded from "line-of-sight" flux from the burst. These remote disturbances are of two types: they are either *prompt* if they occur within a few seconds of the burst and are caused by essentially untrapped particles deflected magnetically into the VLF path, or they are *delayed* if they are caused by geomagnetically trapped particles that drift relatively slowly from the burst region to the VLF path. Delay times for this second class are typically of the order of minutes to tens of minutes.

The perturbation results from the ionization enhancement produced by those particles able to penetrate to D-layer altitudes (70-90 km). Electrons must have energy $E > 50$ keV and protons $E > 1$ MeV to accomplish this. The resulting VLF phase perturbation somewhat resembles a solar-flare perturbation in that the effective ionosphere height is lowered; however, the onset rates are usually considerably higher than those associated with a solar flare, and delayed VLF phase perturbations stemming from nuclear bursts are normally observed only on propagation paths having some portion in darkness.

THE SOVIET BURSTS OF OCTOBER 1962—The Soviet Union exploded two nuclear devices at high altitude over Central Asia during Oct. 1962: at 0341 UT, Oct. 22, and at 0441 UT, Oct. 28, at a point with the coordinates of $\approx 46^\circ$ N and $\approx 72^\circ$ E (corresponding to geomagnetic coordinates of $\approx 36.5^\circ$ N and 149.5° E), as given by Dudziak *et al.*¹¹ Delayed perturbations caused by these bursts were monitored by APL facilities on six separate VLF paths; from these data the types and energies of the particles and the extent of the trapped radiation belts were deduced¹² and compared with satellite particle observations.¹³

We consider that after a high-altitude nuclear burst an artificial radiation belt forms approximately in the geomagnetic meridian through the burst point. The trapped particles forming the belt then drift in the geomagnetic field; the drift

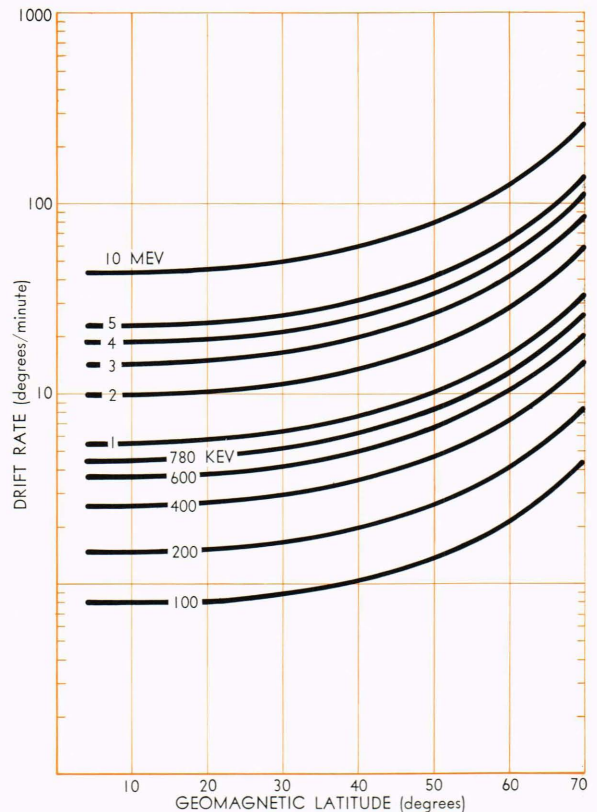


Fig. 5—Calculated drift rates of geomagnetically trapped electrons mirroring at an altitude of 80 km. The curve labeled 780 keV is for the endpoint energy of the neutron-decay beta spectrum.

is eastward for negative particles and westward for positive particles. The rate of drift is a function of particle energy and geomagnetic latitude and is calculated for the dipole field from the expression derived by Hamlin *et al.*,¹⁴ which may be written

$$\omega_d = \frac{3m V^2 (a + h_m)}{eM \sin^2 \theta} f(\theta),$$

where ω_d is the drift rate in rad/sec, m is the relativistic mass and V is the velocity of the particle, a is the earth's radius, h_m is the mirroring altitude (taken as 80 km for VLF altitudes), e is the particle charge, M is the magnetic moment of the earth, θ is the geomagnetic co-latitude of the mirroring point, and $f(\theta)$ is a function of geomagnetic co-latitude that has been evaluated numerically and is tabulated in Ref. 14. Figure 5 shows drift rate as a function of geomagnetic latitude, as calculated from this expression for

¹¹ W. F. Dudziak, D. D. Kleinecke, and T. J. Kostigan, *Graphic Displays of Geomagnetic Geometry*, Report RM 63TMP-2 DSA 1372, General Electric Company, Santa Barbara, Calif., 1963.

¹² C. R. Haave, A. J. Zmuda, and B. W. Shaw, "VLF Phase Perturbations and the Soviet High-Altitude Nuclear Bursts of October 22 and 28, 1962. Part 1. Observations and Inferred Radiation Belts," submitted to *J. Geophys. Res.*

¹³ A. J. Zmuda, C. R. Haave, and B. W. Shaw, "VLF Phase Perturbations and the Soviet High-Altitude Nuclear Bursts of October 22 and 28, 1962. Part 2. Comparison with Satellite Particle Data," submitted to *J. Geophys. Res.*

¹⁴ D. A. Hamlin, R. Karplus, R. C. Vik, and K. M. Watson, "Mirror and Azimuthal Drift Frequencies for Geomagnetically Trapped Particles," *J. Geophys. Res.*, **66**, 1961, 1-4.

electrons of energies between 100 keV and 10 MeV. It is seen that the drift rate increases with both energy and geomagnetic latitude. An energy dispersion thus occurs as the electrons drift eastward from the burst meridian.

The particles of interest here are electrons from the decay of fission fragments and neutron-decay betas. The energy spectra of these two electron species differ in some important respects. The *neutron-decay beta spectrum* contains only electrons of energies up to 0.78 MeV, the endpoint energy as fixed by the mass difference between the neutron and the proton; the relative energy per unit energy interval is maximum for electron energies of about 0.4 MeV. The *fission-beta spectrum* includes electrons of energies up to perhaps 10 MeV; the relative energy per unit energy in-

terval is maximum at about 1 MeV and falls off rapidly for energies above 3.4 MeV. A 4-MeV fission beta at the latitude of APL (51° N, geomagnetic) will drift about four times as fast as a neutron-decay beta having the endpoint energy of 0.78 MeV and about seven times as fast as an 0.4-MeV neutron-decay beta.

Of the six VLF paths monitored, the path from WWVL to APL is perhaps the most interesting from the analysis viewpoint. In this path the effects of electrons from the radioactive decay of fission fragments and from neutron decay are separately shown in the VLF phase perturbations associated with these two Soviet bursts.

Figure 6A shows the phase anomalies recorded on this path for the Soviet bursts of Oct. 22 and 28. Both curves have been normalized to that value of the phase existing just prior to onset of the perturbation. Initial onset time for the burst of Oct. 22 is 6 min. after burst; after starting to recover from this initial perturbation, a second "onset," representing a second lowering of the effective ionosphere height, was observed at $t = 23$ min., after which the relative phase slowly recovers toward its normal value. Only one onset was observed for the Oct. 28 event, at $t = 22$ min. From the scale showing the computed arrival times of electrons of various energies over the WWVL and APL path terminals from the burst meridian, it is seen that the onset at $t = 6$ on Oct. 22 corresponds to the arrival of electrons of energy $3.3 \leq E \leq 3.7$ MeV over the path; the onsets at $t = 22$ on Oct. 28 and $t = 23$ on Oct. 22 correspond closely with the computed arrival time of the 0.78-MeV neutron-decay betas. It is noted here that the time resolution available from the original VLF records was ± 0.5 min. in the timing of specific points (e.g. onset times) so that the energy of the faster moving fission-betas associated with the earlier onset time cannot be fixed as precisely as is possible for the neutron-decay betas.

The first onset on Oct. 22 thus corresponds to the arrival of electrons having energies typical of the fission-beta spectrum; the onsets of 22 and 23 min. relate to the arrival of electrons having the endpoint energy of the neutron-decay beta spectrum.

Figure 6B shows the WWVL-to-APL path in geomagnetic coordinates. The dashed lines show the times (in minutes after burst) at which the "particle front" of electrons having the endpoint energy of the neutron-decay beta spectrum ($E = 0.78$ MeV) is over various points, as computed considering that the belt formed initially in

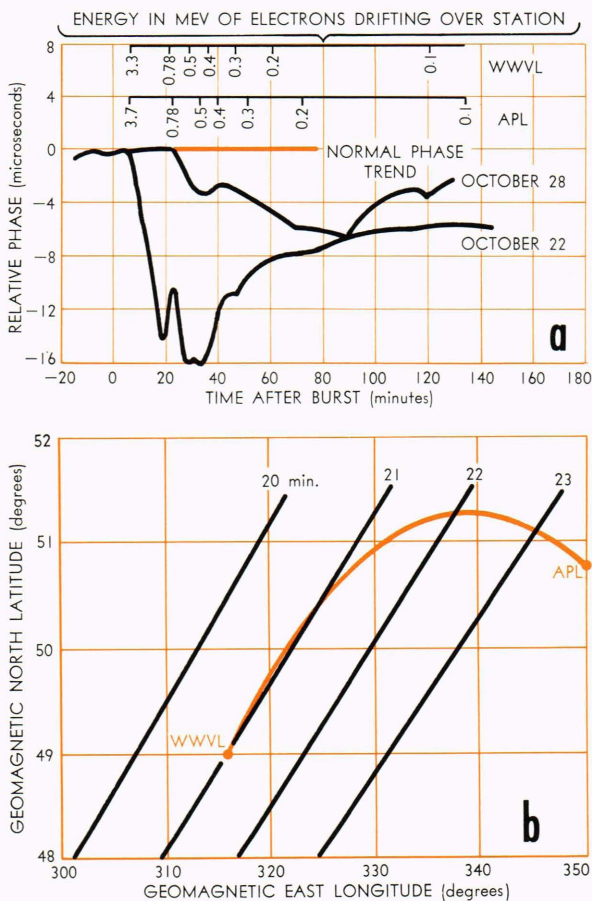


Fig. 6—The WWVL-to-APL path and the Soviet high-altitude bursts of Oct. 1962. (A) Observed phase perturbations. The scales show the computed arrival times of electrons of specific energies over the path terminals. (B) Arrival of neutron-decay betas (780 keV) over the path. The dashed lines show the calculated positions of the particle front at the times indicated.

the geomagnetic meridian through the burst point, 149.5° E. The eastward tilt of the particle front reflects the characteristic that the particles drift more rapidly at higher latitudes. We note that the orientation of the vLF path is such that the 0.78-Mev betas arrive almost simultaneously over all points between WWVL and the point at $\approx 50.5^\circ$ N and 328° E; this represents a path length of about 900 km, or about 40% of the entire path length. At about $t = 23.3$ the 0.78-Mev electrons arrive over APL, and betas of energy 0.68 Mev are over WWVL. The energy range $0.68 < E < 0.78$ Mev, the upper end of the neutron-decay beta energy spectrum, thus brackets the particle energies over the entire path at $t \approx 23$ min.

Electrons with energies characteristic of both the fission-beta and neutron-decay beta spectra were thus present at geomagnetic latitudes between 49° N (WWVL) and 51° N (APL) for the burst of Oct. 22, but only the neutron-decay betas were observed for the Oct. 28 event. This is quite probably caused by a difference in burst altitude, with the later burst being enough lower than the earlier one that the fission betas were confined to latitudes below 49° N.

Figure 7 shows the relationship between the calculated fission-beta fronts and three vLF paths terminating at APL: APL-to-NPM (Hawaii, 19.8 kc/s), APL-to-WWVL and APL-to-GBR. The delayed onset times observed for these paths caused by fission betas were: NPM-to-APL (≈ 5 min.), WWVL-to-APL (6 min.) and GBR-to-APL (6 min.). From Fig. 7 we see that the WWVL-to-APL path and the easternmost portion of the NPM-to-APL path very nearly coincide, and that first contact between the particle fronts and these two paths takes place near the WWVL terminal. Calculated positions of the

particle fronts for 3.5-Mev electrons are shown for $t = 5$ and $t = 6$, and for 4-Mev electrons for $t = 5$. Since the 4-Mev particle front for $t = 5$ is almost identical with a 3.3-Mev front for $t = 6$, the electron-energy range of $3.3 < E < 4$ Mev thus corresponds to the onset times of 5 to 6 min. observed for these two paths. The time resolution available from the vLF records precludes fixing the energy more precisely, but this range (3.3 to 4 Mev) is in good agreement with the energies (energy per unit energy interval) characteristic of the upper end of the fission-beta spectrum from these bursts.

The onset time of $t = 6$ (Oct. 22) on the GBR-to-APL path is seen to correspond with the intersection of particles of these same energies with the path at a latitude of about 55° N. This is interesting in the respect that if these particles had been present in sufficient number at latitudes north of 55° N, an earlier onset than the observed $t = 6$ min. would have been expected. This serves to set the northern limit of the fission-beta belt, insofar as a vLF effect is concerned, at about 55° N for the Oct. 22 burst. No significant perturbation was observed on this path for the Oct. 28 burst, confirming the finding from the WWVL-to-APL path that fission-betas were not present at latitudes north of 49° N for this event and also indicating that the neutron-decay beta belt did not extend significantly north of APL.

A set of delayed vLF perturbations linked with a high-altitude nuclear burst can thus yield substantial information about the geographical extent and the particle species and energies of trapped radiation associated with the burst.

Summary

Largely displaced in the 1920's by HF for communications purposes, vLF in the past five years has experienced a remarkable revival of interest, which is still increasing as newer applications and techniques develop. This resurgence has come about largely through technical advances—notably the stabilization of carrier frequencies with atomic frequency standards—that have enabled certain special characteristics of vLF propagation to be used to advantage in several new applications apart from communications. Very-low-frequency techniques have already become standard practice in the long-range comparison of frequencies. The use of vLF phase measurements for investigating such lower ionosphere phenomena as the nuclear-burst-related D-layer perturbations used here as an example has proved to be a fruitful addition to the tools of ionosphere research.

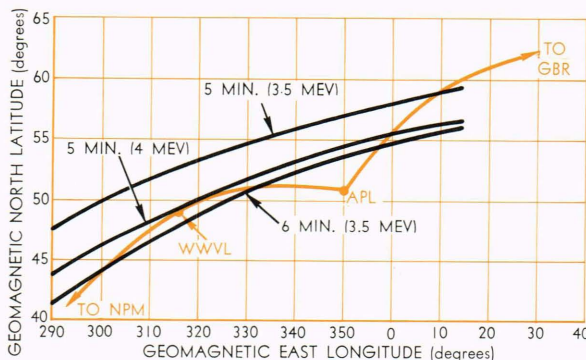


Fig. 7 — Calculated arrival times of fission-beta fronts over vLF paths WWVL-to-APL, GBR-to-APL, and NPM-to-APL.